



Provenance, petrographic and geochemical signatures of sandstones in Çalarasın Formation: A unit of ophiolitic melange in eastern of Kargı District

Cihan Yalçın ¹, Nurullah Hanilçi ², Mustafa Kumral ³, Mustafa Kaya ³

¹Ministry of Industry and Technology, General Directorate of Industrial Zones, Ankara, Türkiye, cihan.yalcin@sanayi.gov.tr

²İstanbul University-Cerrahpaşa, Geological Engineering, İstanbul, Türkiye, nhanilci@gmail.com

³İstanbul Technical University, Geological Engineering, İstanbul, Türkiye, kumral@itu.edu.tr; kayamusta@itu.edu.tr

Cite this study: Yalçın, C., Hanilçi, N., Kumral, M., & Kaya, M. (2022). Provenance, petrographic and geochemical signatures of sandstones in Çalarasın Formation: A unit of ophiolitic melange in eastern of Kargı District. *Engineering Applications*, 1 (2), 145-156

Keywords

Provenance
Geochemical
Sandstone
Çalarasın formation
Central Pontide

Research Article

Received: 28.09.2022

Revised: 28.10.2022

Accepted: 06.11.2022

Published: 14.11.2022



Abstract

Tectonic slices of different origins are observed in the eastern of Kargı (Çorum) district. These slices' metamorphic units and lithologies of ophiolitic melange are observed with tectonic contact. The Çalarasın formation is observed at the upper levels of the ophiolitic mélangé, which extends to the east of Kargı (Çorum) in the Central Pontides. The formation is composed of thin-bedded siltstone intercalated sandstone-shale and mudstone alternations. The sandstones of the formation include quartz, plagioclase, calcite, biotite, chlorite, and volcanic rock particles. The sandstones were analyzed for geochemical properties and provenance traces, respectively. According to these analyzes, SiO₂ % is found between 26.46-71.78%, Al₂O₃% 5.22-10.86, Fe₂O₃% 2.89-7.11 and CaO% 6.13-36.02 respectively. When trace elements are evaluated, Sc content ranges from 76.13-201.03 ppm, and Y content ranges from 9.54-55.11 ppm. Sandstones are rich in large ion lithophile elements (LIL; Ba, Th, U) and poor in high-field strength elements (HFS; Nb, Ti, Zr). Positive anomalies in terms of Pb and Y and negative ones in terms of Eu and P are observed in rocks. The sandstones are poor in terms of REE. The amount of HREE is substantially richer than the amount of LREE. Sandstones were normalized according to PAAS, and a distribution inversely proportional to the primitive values emerged. Ce/Ce* anomaly displays that the same oxygen environment has existed in the environment for a long time, but this situation has changed in the transition zone. Major oxide values suggest that the environment is arid and semi-arid media. It was determined that the sandstones were fed from the intermediate and mafic magmatic sources and tectonically represented the active continental margin and the island arc area.

1. Introduction

By acknowledging the geochemistry of sedimentary rocks, significant data can be obtained about the rocks' tectonic location, geochemical composition, origin, and source area [1-5]. In supplement, environmental interpretations can be represented by acknowledging petrographic characters. In these surveys, sandstones in sedimentary succession are usually preferred.

In the studies to figure out the tectonic origins of the basins, the current states of the most mobile and immobile elements are evaluated [6]. This is expressed by the values of both major oxides and trace elements. In particular, trace elements show the characteristics of the major source (tectonic environments and source-rock compositions) during weathering and transportation [2, 4, 7]. Rare earth elements are also used to characterize the source and tectonic environment of the sedimentation [8-11]. As a result of all these evaluations, interpretations are made corresponding to the geochemical data of the sedimentary rock. For example, elemental ratios such as La/Sc, La/Co, and Th/Sc are preferred for separating mafic and felsic source rocks [12]. It is noted that trace elements such as La and Th are more concentrated in felsic igneous rocks, while Co, Sc and Cr have

higher concentrations in mafic rocks [10-11, 13]. All accepted elemental analysis results are evaluated closely, and a sedimentary rock's origin and tectonic environment are interpreted.

Pontides were established as part of the Alpine-Himalayan belt by Ketin [14], and Okay et al. [15] separated it into Istanbul, Strandja, and Sakarya zones, respectively. The Pontides are geographically distributed as western, central, and eastern Pontides. Yilmaz et al. [16] stated that the Pontides are the orogenic belt related to the opening and closing of the Tethys Ocean in the northernmost part of Turkey. As a result of this tectonic movement, a submarine turbidite basin was formed in the Central Pontides during the Early Cretaceous [17].

The Central Pontides consist of metamorphic, magmatic, and sedimentary rock groups in the Late Paleozoic-Early Cenozoic age range along the 'suture zones' formed by the closure of the Paleo-Tethys and Neotethys oceans [18-25]. Ustaömer and Robertson [26] stated that the metamorphic rocks in the area they call the Domuzdağ-Saraycıkdağı complex in the region have undergone metamorphism in the blueschist facies and the regressive greenschist facies.

East of Kargı (Gökçedoğan), located in the Central Pontides, specific tectonostratigraphic sequences dwelling in lower and upper tectonic slices [27]. These slices are Pelitözü, Gölköy, and ophiolitic melange slices, respectively [28-29]. In the upper levels of the ophiolitic mélangé, the Çalarasın formation consists of sedimentary rocks. This paper highlights the provenance diagnosis and geotectonic environment interpretations of the sandstones of the Çalarasın formation by revealing the petrographic and geochemical studies.

2. Material and Method

Thin sections and geochemical analyzes of 7 samples collected from sandstones in the Çalarasın formation were performed in ITU-JAL. Geochemical analyzes consist of major oxide (Table 1), trace element (Table 2), and rare earth element values (Table 3). The analysis results obtained were evaluated in different diagrams. In addition, REE results were normalized according to PAAS (Table 4) and compared in the spider diagram. The analysis results in question are given in Table 1. In addition, the ratios and anomalies of critical elements for the diagnosis of geotectonic environment and provenance were determined.

2.1. Geological framework

The study area is located in a district where the Middle Jurassic and Cretaceous accretionary prism is still called the Central Pontides Supercomplex [30-32]. To the east of Kargı is the Middle Jurassic accretionary complex, which has the Kirazbaşı complex consisting of ophiolitic mélangé, and the Domuzdağ complex, whose metamorphic conditions change towards the north [33-34].

Autochthonous and allochthonous rock groups are observed together in the study area (Figure 1). Kunduz metamorphics are observed at the base of the region. This metamorphic unit is overlain by Permian aged Çamdağ and Jura-Cretaceous aged İnaltı formation with tectonic contact. In addition, in a large part of the study area, the lithologies of the Ophiolitic Melange overlie the Kunduz metamorphics with a tectonic contact. With these thrust contacts, tectonic slices were formed in the region [29]. On these slices, Beşpınar, Yedikır, and Ilgaz formations and Quaternary alluviums are observed with angular unconformity (Figure 1).

2.2. Ophiolitic melange

The Ophiolitic Melange of the Kirazbaşı complex consists of dunite and serpentinite at the base, spilitic lava, metadiabase, metabasalt, radiolarite, chert, mudstone, and pelagic limestones [33, 34] on the gabbro. At the top levels of the succession, there is the Çalarasın formation [35], which consists of alternating siltstone, sandstone, shale, and mudstone, respectively (Figure 2).

In addition, conglomerate-gravelly sandstone layers without lateral continuity are also observed in this unit. In the steep topography, whitish-grey, cream-colored medium-thick bedded limestone olistoliths of varying sizes are seen at different unit levels.

The sandstones observed in the vicinity of the Çalarasın district are brownish, reddish grey on the weathered surface, bright black in areas where the fresh fracture surface is altered, and brown and grey in localities where alteration is observed, unstable, medium-hard, fossil-free, poorly sorted and ungraded.

2.3. Petrography

In the thin section review of the sandstones in Beşpınar, it is recognized that there are many volcanic rock fragments in the rock. There are mainly quartz, plagioclase, calcite, and rock particles. Grains are medium well, rounded, poorly sorted, and ungraded. Quartz exists as monocrystalline. Calcite is in the matrix, and secondary quartz and iron oxide minerals are emplaced in its fractures and cracks. It was observed to be fed from volcanic rocks during the deposition (Figure 3).

Corresponding to Folk [36], the rock was determined as lithic arenite because the quartz content is less than 90%, the rock particle is more than feldspar, and the matrix ratio is less than 15%.

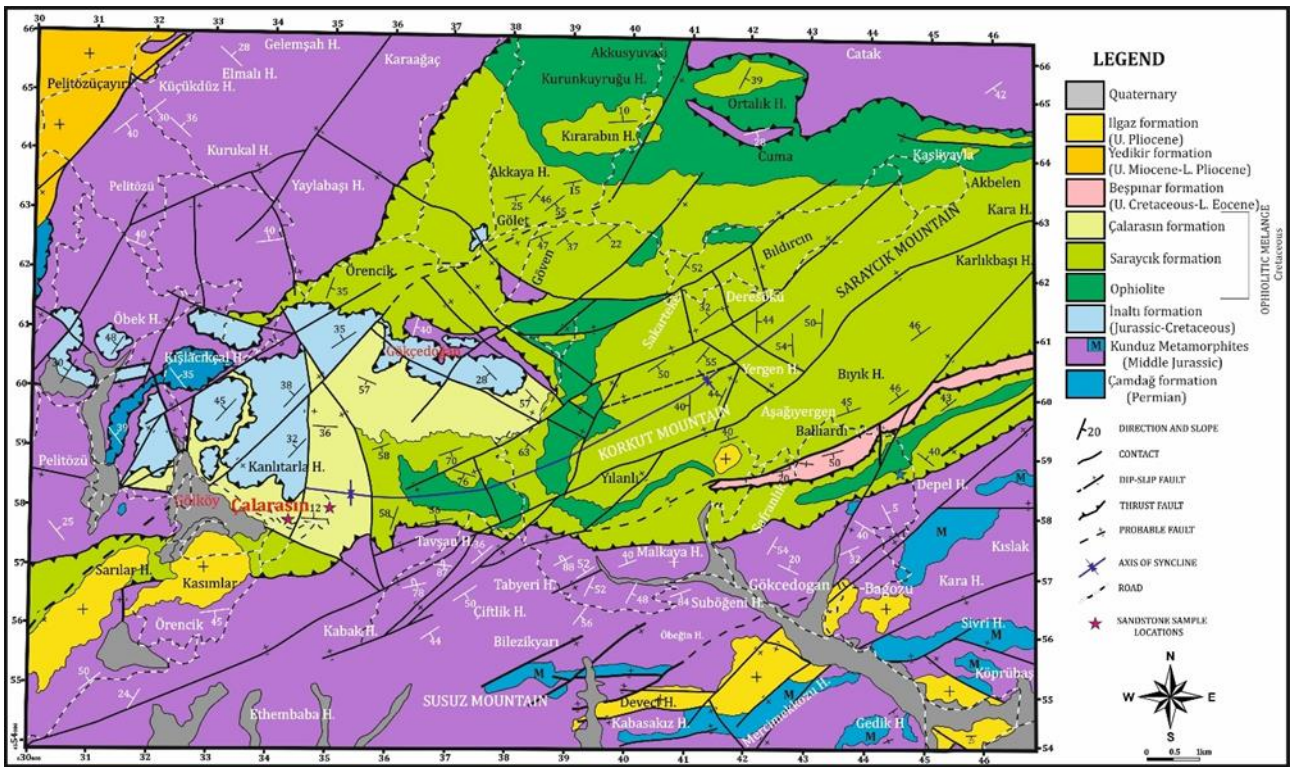


Figure 1. Geological map of the study area (Modified from Yalçın et al., [29])



Figure 2. General view of the Çalarasin formation (South to North View)

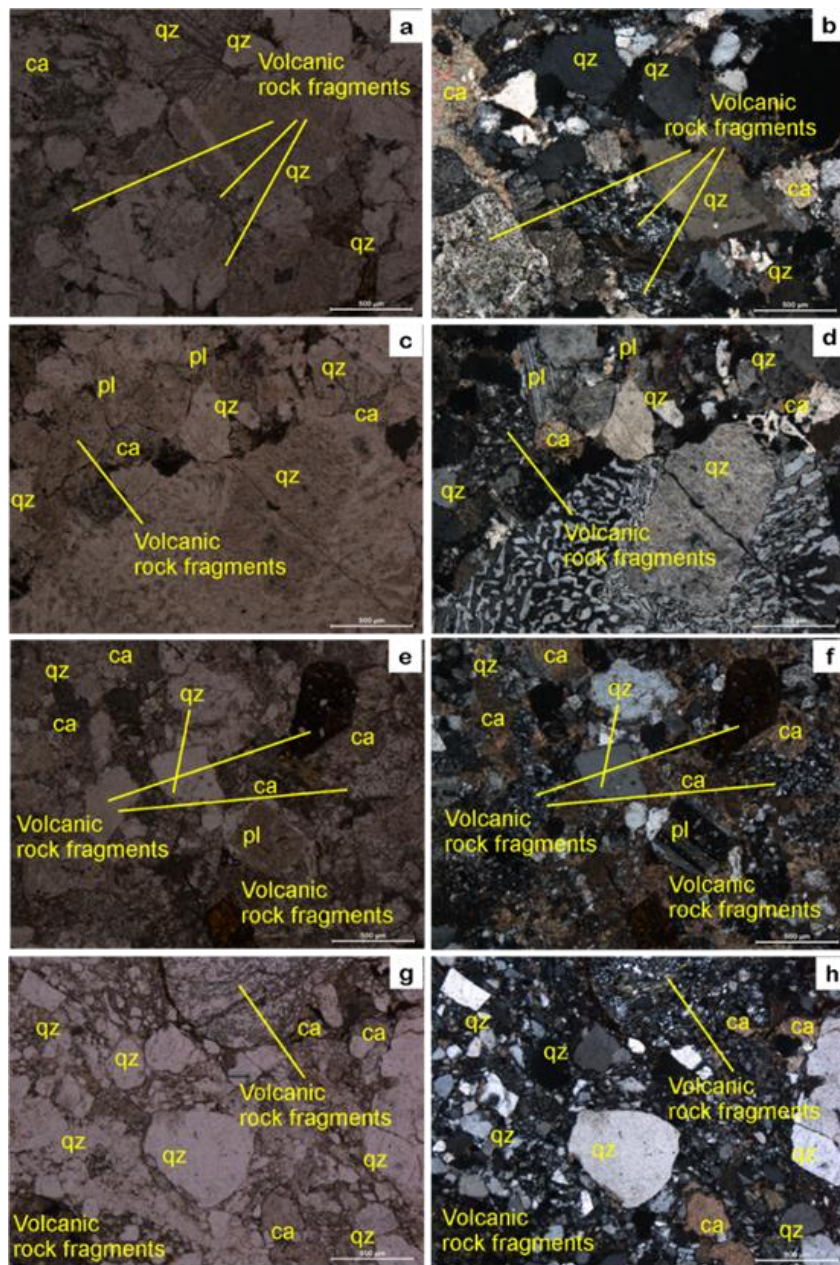


Figure 3. Polarizing microscope images of the sandstones of the Çalarasin formation Abbreviations: ca: calcite; qz: quartz; pl: plagioclase)

Table 1. Major oxides (%wt) concentrations of the sandstones

ROCK	Sandstone	Sandstone	Sandstone	Sandstone	Sandstone	Sandstone	Sandstone
SAMPLE	KGD-9	KGD-10	KGD-12	KGD-13	KGD-14	KGD-15	KGD-20
Latitude (°N)	34.630	34.600	34.606	34.630	34.630	34.630	34.606
Longitude (°E)	58.020	57.990	57.990	58.020	58.020	58.020	57.970
Major Oxides (%)							
SiO ₂	71,78	52,72	62,91	26,46	69,02	56,34	62,86
Al ₂ O ₃	9,22	6,45	10,18	6,71	5,22	7,10	10,86
Fe ₂ O ₃	2,89	3,13	5,55	1,77	3,55	3,45	7,11
MgO	1,09	0,89	1,86	0,76	0,77	1,15	2,67
CaO	6,13	20,43	9,55	36,02	13,22	18,52	6,80
Na ₂ O	3,28	1,54	2,68	0,69	0,55	2,12	2,76
K ₂ O	0,60	0,70	0,75	1,18	0,76	0,56	0,90
TiO ₂	0,27	0,26	0,35	0,32	0,30	0,22	0,59
P ₂ O ₅	0,09	0,10	0,10	0,06	0,09	0,05	0,08
MnO	0,05	0,37	0,09	0,07	0,05	0,24	0,11
Cr ₂ O ₃	0,00	0,00	0,00	0,01	0,01	0,00	0,00
LOI	4,41	13,2	5,82	25,76	6,34	10,05	5,03
Total	99,82	99,78	99,84	99,81	99,98	99,81	99,76

Table 2. Trace element concentrations (ppm) of the sandstones

ROCK	Sandstone	Sandstone	Sandstone	Sandstone	Sandstone	Sandstone	Sandstone
SAMPLE	KGD-9	KGD-10	KGD-12	KGD-13	KGD-14	KGD-15	KGD-20
Trace elements							
Sc	201,03	149,44	167,43	76,13	198,97	115,85	131,56
Y	55,11	11,76	11,47	15,83	10,01	14,16	9,54
Th	0,73	9,26	2,48	6,03	3,01	2,48	2,22
Li	23,88	38,81	35,14	11,65	27,72	27,40	40,02
Be	1,57	0,89	0,85	1,90	1,09	1,52	1,31
Co	39,98	13,49	15,60	30,59	12,25	18,18	15,39
Ni	61,88	61,27	27,48	35,99	18,85	36,41	51,95
Cu	69,70	0,00	0,00	0,00	0,00	0,00	0,00
Zn	369,21	0,00	0,00	0,00	0,00	0,00	0,00
Ga	22,50	20,06	14,66	11,97	7,78	11,77	24,71
As	39,93	42,54	37,15	42,72	32,58	32,89	33,02
Se	16,15	38,02	4,41	18,96	0,00	10,46	0,00
Rb	16,38	21,70	18,69	46,46	20,66	16,13	17,17
Sr	298,92	246,47	101,17	237,35	148,96	224,09	97,19
Ag	8,71	3,26	0,76	0,81	0,51	0,49	0,85
Cd	0,51	0,18	0,00	0,46	0,03	0,09	0,00
In	0,42	0,60	0,20	0,15	0,07	0,00	0,08
Cs	2,03	0,85	0,57	2,37	0,71	0,35	0,41
Ba	134,32	461,23	199,42	137,94	89,08	171,43	541,86
Tl	0,24	0,03	0,08	0,26	0,04	0,05	0,03
Pb	37,88	0,00	0,00	120,80	0,23	13,49	28,00
U	0,00	1,36	0,58	2,79	0,79	0,64	0,68
Au	0,09	0,02	0,04	0,06	0,03	0,03	0,02
Hf	8,57	1,29	0,99	0,23	0,81	0,81	1,17
Ir	0,07	0,01	0,03	0,01	0,01	0,02	0,02
Pd	1,09	2,61	1,83	0,57	1,84	1,47	2,29
Pt	0,12	0,02	0,02	0,00	0,01	0,04	0,02
Rh	0,07	0,05	0,03	0,05	0,04	0,05	0,04
Ru	0,06	0,23	0,18	0,15	0,21	0,23	0,22
Sb	0,50	3,14	0,86	2,07	0,86	2,90	3,58
Sn	1,73	1,16	1,07	1,52	1,03	0,92	1,14
Te	0,01	0,07	0,12	0,04	0,05	0,06	0,09

3. Geochemistry

As a result of the analysis, the %SiO₂ changes of the sandstones in the Çalarasın formation are between 26.46-71.78. It is recognized that the example with low SiO₂ content is carbonate-rich carbonate sandstone. In petrographic studies, it has been determined that sandstones are usually carbonate cemented and rich in volcanic rock particles. Al₂O₃ values range between 5.22-10.86%, Fe₂O₃ values between 2.89-7.11%, and CaO values between 6.13-36.02%. There is no significant difference in the samples regarding Na₂O, K₂O, P₂O₅, TiO₂, and MnO, respectively. When trace elements are evaluated, it is seen that the Ba, Sc, and Sr ratios of the samples are high. It is seen that the Ba content reaches up to 541.86 ppm. Sc content varies between 76.13-201.03 ppm, and Sr content ranges between 97.19-298.92 ppm.

According to the chondrite normalized trace element spider diagram of the sandstones [37], it is observed that there is enrichment with large ion lithophile elements (LILE; Ba, Th, U) (Figure 4). Elements with high-field strength elements (HFSE; Nb, Ti, Zr) show depletion. Positive Pb and Y anomalies are observed in the rocks. A negative anomaly is observed in terms of Eu and P. The enrichment in Th indicates that heavy minerals containing Th are situated in the volcanic rock particle.

A Rare Earth Element (REE) spider diagram [38] normalized to the Chondrite of sandstones was prepared (Figure 5). At the same time, the values normalized according to PAAS are shown in the same diagram. According to the diagram, enrichment by Light Rare Earth Elements (LREE; La, Ce, Pr, Nd) and a horizontal and near-

horizontal distribution was observed for Heavy Rare Earth Elements (HREE; Er, Tm, Yb, Lu) for sandstones. There is a negative anomaly in terms of Eu content. However, the values normalized according to PAAS show an inverse proportional distribution compared to the normalized values (Figure 5).

Table 3. REE concentrations (ppm) and some ratios of the sandstones

ROCK	Sandstone	Sandstone	Sandstone	Sandstone	Sandstone	Sandstone	Sandstone
SAMPLE	KGD-9	KGD-10	KGD-12	KGD-13	KGD-14	KGD-15	KGD-20
Rare Earth Elements							
La	6,81	10,56	7,42	11,69	8,05	8,11	5,61
Ce	20,59	21,24	15,32	22,89	16,30	15,24	11,92
Pr	3,50	2,34	1,85	2,89	2,11	1,78	1,46
Nd	18,88	9,23	7,43	11,03	8,63	7,18	5,99
Sm	6,44	2,47	2,06	2,33	2,12	1,85	1,92
Eu	2,15	0,83	0,60	0,51	0,57	0,52	0,68
Gd	9,72	3,14	2,73	2,81	2,85	2,62	2,20
Tb	1,62	0,38	0,36	0,37	0,35	0,36	0,30
Dy	10,71	2,11	2,10	2,30	1,87	2,30	1,75
Ho	2,26	0,42	0,45	0,50	0,38	0,50	0,38
Er	6,79	1,14	1,27	1,59	1,00	1,50	1,11
Tm	0,97	0,16	0,19	0,23	0,13	0,22	0,16
Yb	6,14	1,03	1,23	1,54	0,82	1,44	1,08
Lu	0,92	0,16	0,20	0,24	0,12	0,22	0,18
Σ REE	97,49	55,23	43,22	60,90	45,30	43,84	34,74
Σ LREE	58,36	46,67	34,70	51,33	37,78	34,67	27,58
Σ HREE	39,13	8,56	8,53	9,58	7,52	9,17	7,15
Ce/Ce*	0,31	0,74	0,65	0,76	0,64	0,70	0,59
Eu/Eu*	1,26	1,40	1,19	0,93	1,08	1,11	1,55
Th/Sc	0,00	0,06	0,01	0,08	0,02	0,02	0,02
La/Sc	0,10	1,25	0,58	0,78	0,21	0,80	2,14
La/Co	0,30	7,31	2,65	3,65	1,18	2,98	10,94
Th/Co	4,31	7,43	6,06	5,66	7,54	5,27	5,85
Ba/Sc	0,33	0,20	0,22	0,20	0,21	0,25	0,20
Ba/Co	0,93	1,17	1,03	0,95	1,19	0,94	1,02

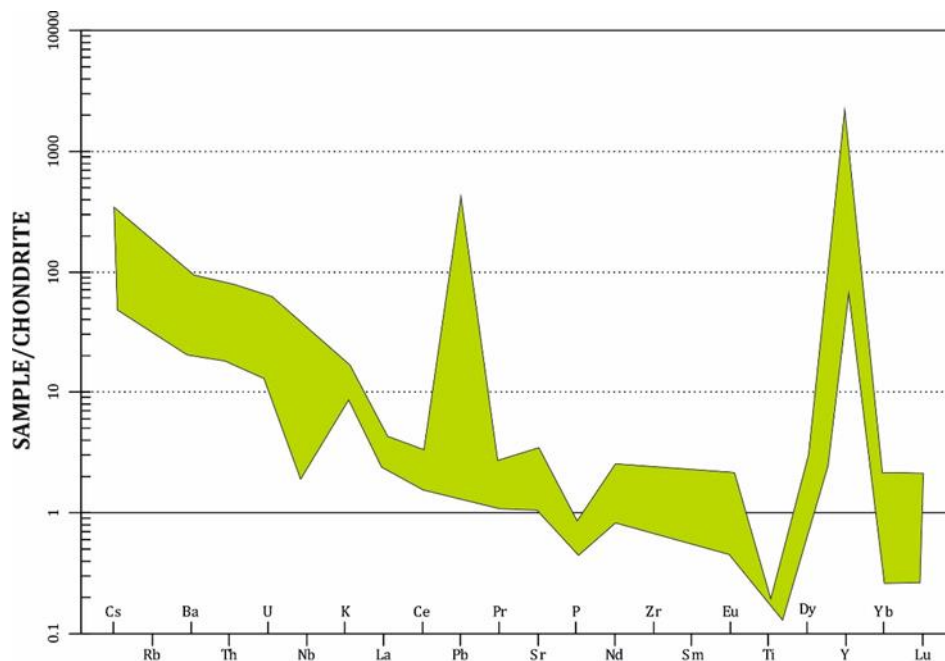


Figure 4. Spider diagram of chondrite-normalized trace and REE elements

Table 4. PAAS normalized REE concentrations (ppm) of the sandstones

ROCK	Sandstone	Sandstone	Sandstone	Sandstone	Sandstone	Sandstone	Sandstone
SAMPLE	KGD-9	KGD-10	KGD-12	KGD-13	KGD-14	KGD-15	KGD-20
La	0,178	0,276	0,194	0,306	0,211	0,212	0,147
Ce	0,259	0,267	0,192	0,288	0,205	0,192	0,150
Pr	0,396	0,265	0,210	0,327	0,239	0,201	0,166
Nd	0,557	0,272	0,219	0,325	0,255	0,212	0,177
Sm	1,161	0,445	0,372	0,420	0,382	0,333	0,346
Eu	1,987	0,773	0,560	0,472	0,529	0,485	0,633
Gd	2,085	0,674	0,585	0,603	0,612	0,562	0,472
Tb	2,098	0,495	0,461	0,473	0,449	0,468	0,386
Dy	2,287	0,452	0,449	0,492	0,400	0,492	0,374
Ho	2,276	0,426	0,454	0,501	0,382	0,502	0,380
Er	2,384	0,401	0,447	0,558	0,352	0,527	0,388
Tm	2,395	0,404	0,472	0,576	0,333	0,538	0,396
Yb	2,176	0,365	0,437	0,546	0,290	0,512	0,383
Lu	2,135	0,373	0,451	0,553	0,270	0,513	0,413

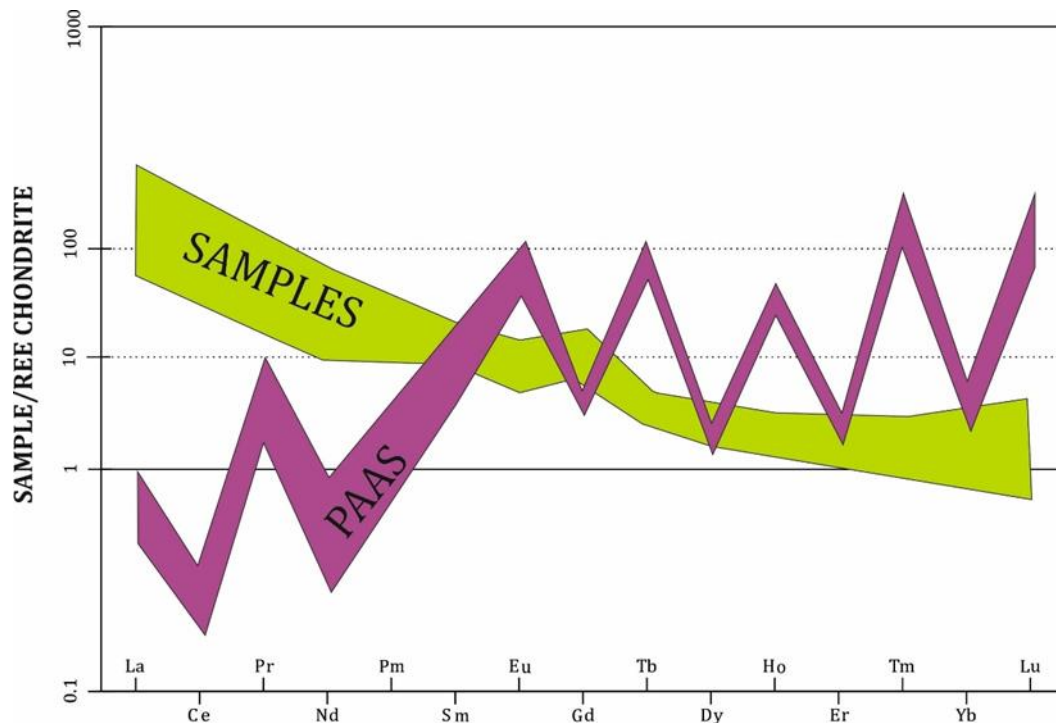


Figure 5. Spider diagram of chondrite and PAAS normalized REE elements

Ce anomaly is a parameter used to determine the redox conditions of the environment [39]. Ce is found in trivalent terrestrial sedimentary and igneous rocks [40]. In addition, different cations of Ce are found in seawater in anoxic or suboxic environments [41]. According to these Ce values, the environment can be interpreted. A diagram was prepared to reveal the Ce anomalies of the sandstone (Figure 6). According to this diagram, it can be said that although the amount of oxygen in the deposition environment remains the same for a long time, there is some change in the transition zone.

4. Provenance

To reveal the provenance traces of the sandstones, the diagram was prepared using the main oxide values [42]. According to the prepared diagram, it was determined that the sandstones were fed from intermediate and mafic magmatic sources (Figure 7).

To determine the geotectonic environment of the sandstones, a change diagram based on the first and second differentiation functions proposed by Bhatia [1] was prepared (Figure 8). According to the prepared diagram, 3 of the samples fall in the passive margin area, 3 in the continental arc area, and 1 in the island arc area.

According to the diagram of Suttner and Dutta [43], which was prepared according to the major oxide values, the rocks were formed in semi-arid and arid environment conditions (Figure 9). 1 sample reflects the humid environmental conditions.

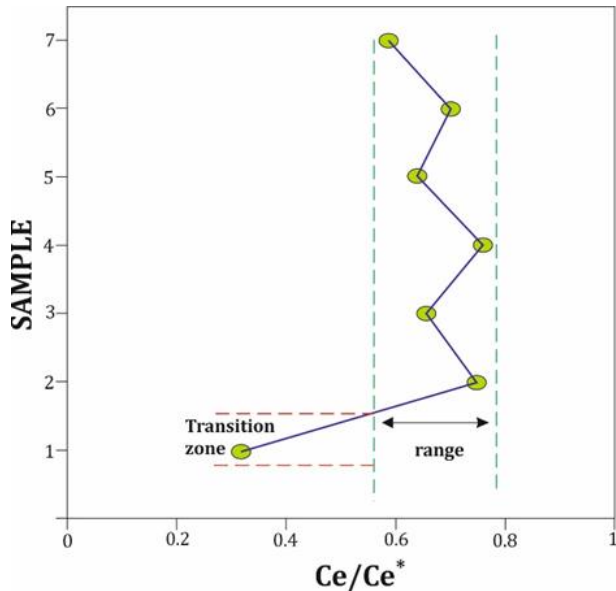


Figure 6. Ce anomaly variations of sandstones

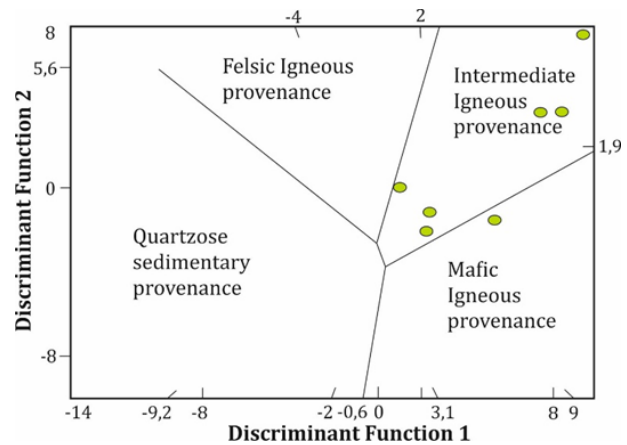


Figure 7. Geotectonic discrimination diagram for the provenance of sandstones by major elements [42]

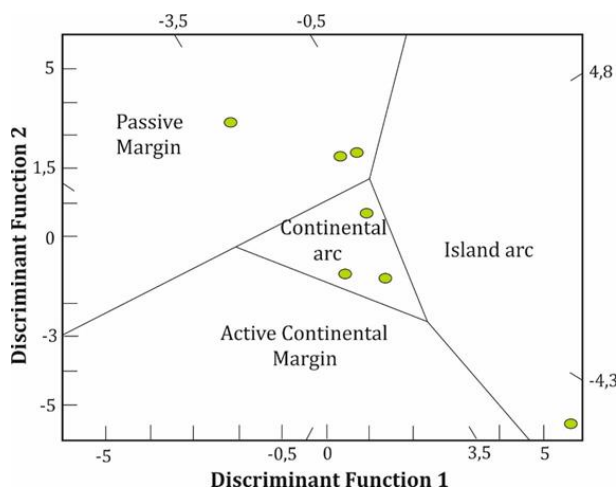


Figure 8. F1-F2 discriminant function diagram of sandstones [1]

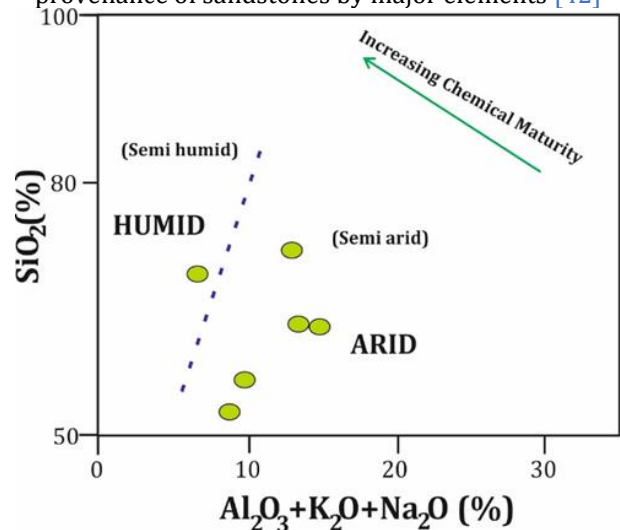


Figure 9. Chemical maturity of sandstone [43]

For sandstones, most of the samples examined in the $(\text{Fe}_2\text{O}_3+\text{MgO})-\text{TiO}_2$ diagram [1] are distributed outside the defined areas (Figure 10a). Only one specimen is located in the active continental margin area. In the $(\text{Fe}_2\text{O}_3+\text{MgO})-(\text{Al}_2\text{O}_3/\text{SiO}_2)$ diagram [1], many samples fall into the active continental margin area (Figure 10b). In the La/Th variation diagram developed by Bhatia and Crook [2], the samples fall into the island arc area (Figure 10c), and in the Th-Co-Zr/10 diagram (Figure 10d), the samples fall into the island arc area.

Th and Sc are important and useful elements in provenance interpretations [8]. In addition, Eu anomalies have a critical role in the diagnosis of provenance. For this reason, Eu anomaly and compositional variations [44] of magmatic origin rocks were evaluated together in the Th/Sc diagram [45] (Figure 11). It has been determined that some of the sandstones exhibit a similar distribution to the basaltic composition and some present different characteristics. In addition, strategically important La/Sc, La/Co, Th/Co, Ba/Sc, Ba/Co, and Th/Sc ratios were determined and correlated according to the compositional variations of granitic and volcanic rocks [44]. These data show that the sandstones are fed from basaltic composition, but some are from rocks of different characteristics.

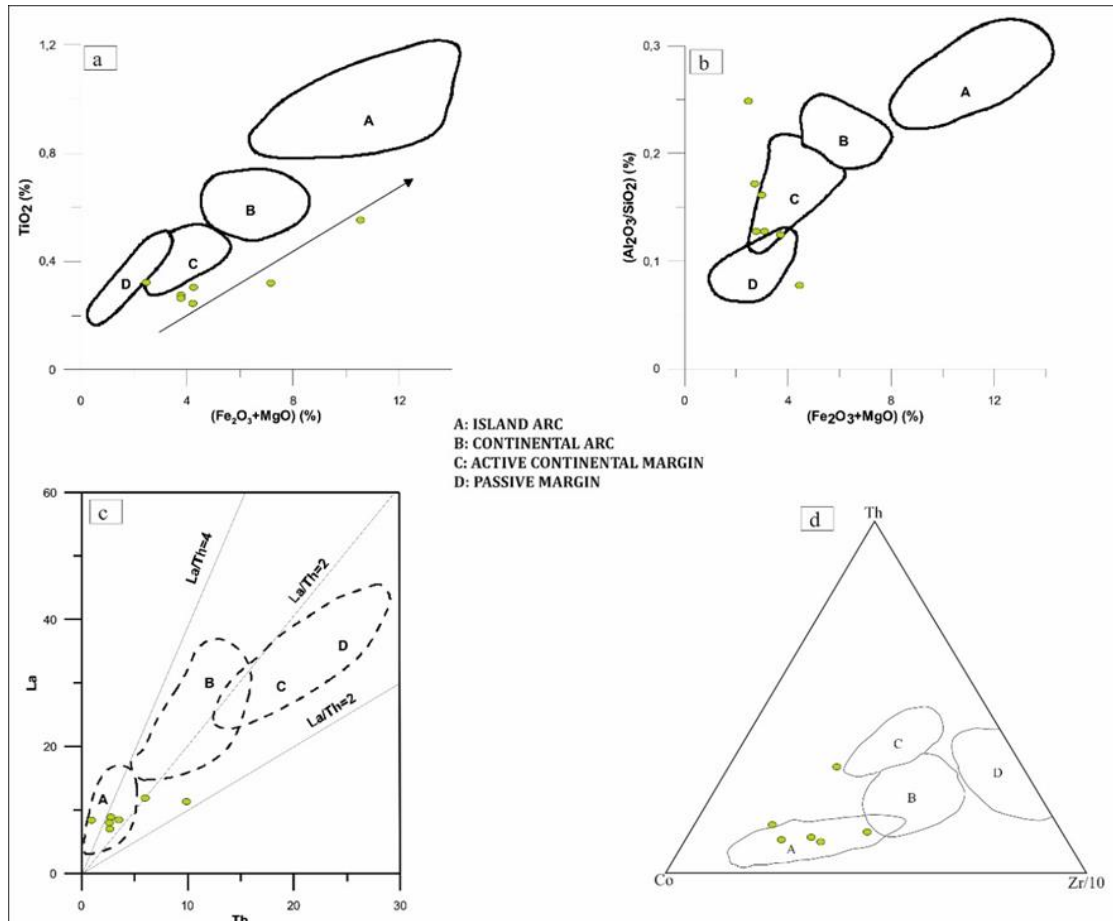


Figure 10. Geotectonic diagrams of sandstones

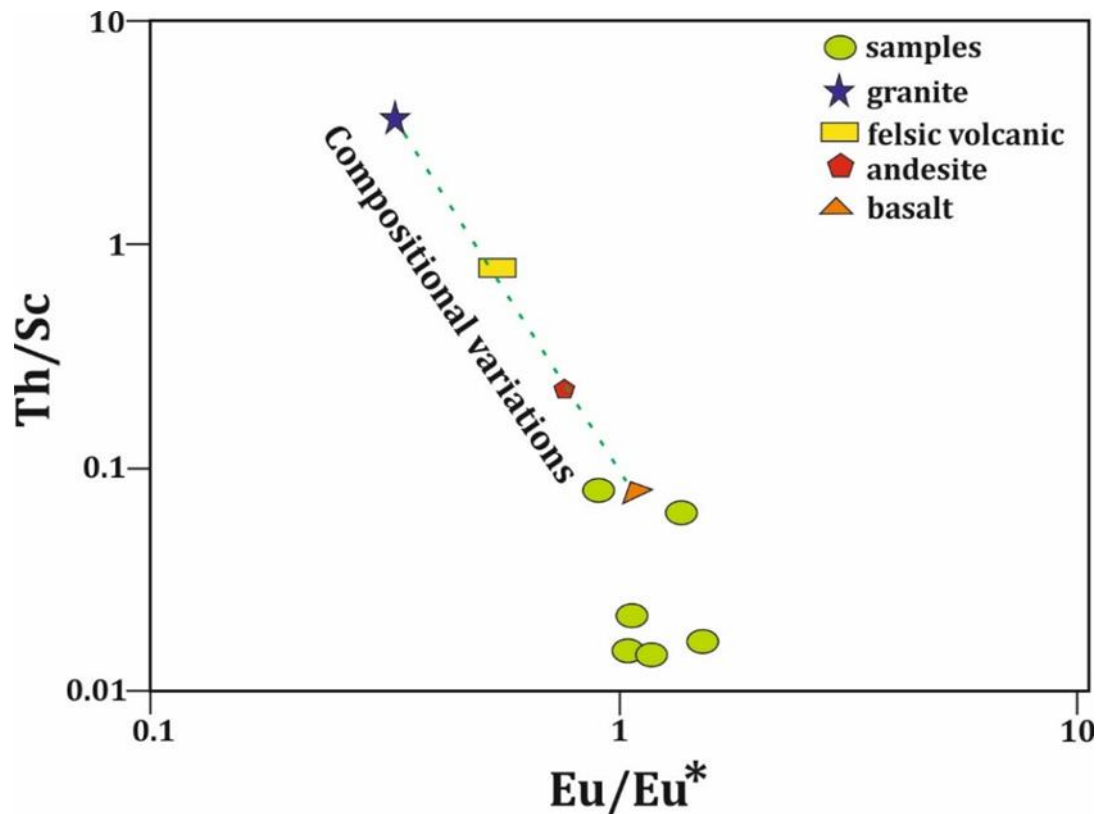


Figure 11. Chemical Eu/Eu^* - Th/Sc binary diagram [46]

5. Conclusion

The petrographic and geochemical properties of the sandstones, which are located in a very complex area and represent the upper levels of the lithologies belonging to the ophiolitic melange, have been revealed. As a result of the study, it was determined that the sandstones defined as lithic arenite were fed from intermediate and mafic magmatic sources and concentrated in the tectonically active continental area and island arc area.

When sandstones poor in REE are normalized according to PAAS, a distribution inversely proportional to the primary situation emerges. Ce anomaly shows that the same oxygen environment has existed in the environment for a long time, but this situation has changed somewhat in the transition zone.

In the $\text{SiO}_2\text{-Al}_2\text{O}_3\text{+Na}_2\text{O+K}_2\text{O}$ diagram, it was determined that the environment was arid and semi-arid. The amount of HREE is considerably higher than the amount of LREE. La/Sc, La/Co, Th/Co, Ba/Sc, Ba/Co, and Th/Sc ratios, which have critical roles in provenance studies, were determined and compared with the compositions of granitic and volcanic rocks. According to these results, it has been determined that the sandstones reflect a unique characteristic. Isotope studies should be done for more detailed interpretations.

Acknowledgement

This study is part of a Ph.D. thesis prepared in the Graduate School of Science and Engineering of İstanbul University and supported by TUBITAK project no: 113Y536. This study was partly presented at the 4th Advanced engineering Days [47] on 21 September 2022.

Funding

This research received no external funding.

Author contributions:

Cihan Yalçın: Writing-Reviewing and Editing, Geology, Methodology, Geochemistry. **Nurullah Hanilçi:** Editing, Geochemistry. **Mustafa Kumral:** Petrography, **Mustafa Kaya:** Petrography, XRF/ICP-MS

Conflicts of interest

The authors declare no conflicts of interest.

References

1. Bhatia, M. R. (1983). Plate tectonics and geochemical composition of sandstones. *The Journal of Geology*, 91(6), 611-627.
2. Bhatia, M. R., & Crook, K. A. (1986). Trace element characteristics of graywackes and tectonic setting discrimination of sedimentary basins. *Contributions to mineralogy and petrology*, 92(2), 181-193.
3. Roser, B. P., & Korsch, R. J. (1988). Provenance signatures of sandstone-mudstone suites determined using discriminant function analysis of major-element data. *Chemical geology*, 67(1-2), 119-139.
4. McLennan, S. M. (2018). Rare earth elements in sedimentary rocks: influence of provenance and sedimentary processes. In *Geochemistry and mineralogy of rare earth elements* (pp. 169-200).
5. Armstrong-Altrin, J. S., & Verma, S. P. (2005). Critical evaluation of six tectonic setting discrimination diagrams using geochemical data of Neogene sediments from known tectonic settings. *Sedimentary Geology*, 177(1-2), 115-129.
6. Armstrong-Altrin, J. S., Lee, Y. I., Verma, S. P., & Ramasamy, S. (2004). Geochemistry of sandstones from the Upper Miocene Kudankulam Formation, southern India: implications for provenance, weathering, and tectonic setting. *Journal of sedimentary Research*, 74(2), 285-297.
7. Condie, K. C., Boryta, M. D., Liu, J., & Qian, X. (1992). The origin of khondalites: geochemical evidence from the Archean to early Proterozoic granulite belt in the North China craton. *Precambrian Research*, 59(3-4), 207-223.
8. Taylor, S. R., & McLennan, S. M. (1985). The continental crust: its composition and evolution: an examination of the geological record preserved in sedimentary rocks. Oxford, U.K., Blackwell, 328 pages.
9. Wronkiewicz, D. J. (1989). Geochemistry and provenance of sediments from the Pongola Supergroup, South Africa: evidence for a 3.0-Ga-old continental craton. *Geochimica et Cosmochimica Acta*, 53(7), 1537-1549.
10. Wronkiewicz, D. J., & Condie, K. C. (1987). Geochemistry of Archean shales from the Witwatersrand Supergroup, South Africa: source-area weathering and provenance. *Geochimica et Cosmochimica Acta*, 51(9), 2401-2416.

11. Wronkiewicz, D. J., & Condie, K. C. (1990). Geochemistry and mineralogy of sediments from the Ventersdorp and Transvaal Supergroups, South Africa: cratonic evolution during the early Proterozoic. *Geochimica et Cosmochimica Acta*, 54(2), 343-354.
12. Tijani, M. N., Nton, M. E., & Kitagawa, R. (2010). Textural and geochemical characteristics of the Ajali Sandstone, Anambra Basin, SE Nigeria: implication for its provenance. *Comptes Rendus Geoscience*, 342(2), 136-150.
13. Ronov, A. B., Balashov, Y. A., Girin, Y. P., Bratishko, R. K., & Kazakov, G. A. (1974). Regularities of rare-earth element distribution in the sedimentary shell and in the crust of the earth. *Sedimentology*, 21(2), 171-193.
14. Ketin, İ. (1966). Tectonic units of Anatolia (Asia minor). *Bulletin of the Mineral Research and Exploration*, 66(66), 24-34.
15. Okay, A. I., Celal Sengor, A. M., & Görür, N. (1994). Kinematic history of the opening of the Black Sea and its effect on the surrounding regions. *Geology*, 22(3), 267-270.
16. Yılmaz, Y., Tüysüz, O., Yigitbas, E., Genç, S.C. & Şengör, A.M.C., (1997). Geology and tectonic evolution of the Pontides, in Robinson, A.G. (ed). Regional and Petroleum Geology of the Black Sea and Surrounding Region, vol. 68. Bulletin of American Association Petroleum Geology, pp. 183-226.
17. Akdoğan, R., Okay, A. I., Sunal, G., Tari, G., Meinhold, G., & Kylander-Clark, A. R. (2017). Provenance of a large Lower Cretaceous turbidite submarine fan complex on the active Laurasian margin: Central Pontides, northern Turkey. *Journal of Asian Earth Sciences*, 134, 309-329. <https://doi.org/10.1016/j.jseaes.2016.11.028>.
18. Robertson, A. H. (2002). Overview of the genesis and emplacement of Mesozoic ophiolites in the Eastern Mediterranean Tethyan region. *Lithos*, 65(1-2), 1-67.
19. Robertson, A. H., & Ustaömer, T. (2004). Tectonic evolution of the Intra-Pontide suture zone in the Armutlu Peninsula, NW Turkey. *Tectonophysics*, 381(1-4), 175-209.
20. Robertson, A. H., Ustaömer, T., Parlak, O., Ünlügenç, U. C., Taşlı, K., & Inan, N. (2006). The Berit transect of the Tauride thrust belt, S Turkey: Late Cretaceous–Early Cenozoic accretionary/collisional processes related to closure of the Southern Neotethys. *Journal of Asian Earth Sciences*, 27(1), 108-145.
21. Okay, A. I., Tüysüz, O., Satır, M., Ozkan-Altiner, S., Altiner, D., Sherlock, S., & Eren, R. H. (2006). Cretaceous and Triassic subduction-accretion, high-pressure–low-temperature metamorphism, and continental growth in the Central Pontides, Turkey. *Geological Society of America Bulletin*, 118(9-10), 1247-1269.
22. Okay, A. I., Sunal, G., Sherlock, S., Alt ner, D., Tüysüz, O., Kylander-Clark, A. R., & Aygül, M. (2013). Early Cretaceous sedimentation and orogeny on the active margin of Eurasia: Southern Central Pontides, Turkey. *Tectonics*, 32(5), 1247-1271.
23. Okay, A. I., & Nikishin, A. M. (2015). Tectonic evolution of the southern margin of Laurasia in the Black Sea region. *International Geology Review*, 57(5-8), 1051-1076.
24. Aygül, M., Okay, A. I., Oberhaensli, R., Schmidt, A., & Sudo, M. (2015). Late Cretaceous infant intra-oceanic arc volcanism, the Central Pontides, Turkey: petrogenetic and tectonic implications. *Journal of Asian Earth Sciences*, 111, 312-327. <https://doi.org/10.1016/j.jseaes.2015.07.005>.
25. Aygül, M., Okay, A. I., Oberhänsli, R., & Sudo, M. (2016). Pre-collisional accretionary growth of the southern Laurasian active margin, Central Pontides, Turkey. *Tectonophysics*, 671, 218-234.
26. Ustaömer, T., & Robertson, A. H. (1999). Geochemical evidence used to test alternative plate tectonic models for pre-Upper Jurassic (Palaeotethyan) units in the Central Pontides, N Turkey. *Geological Journal*, 34(1-2), 25-53.
27. Uğuz, M.F. & Sevin, M. (2009). 1/100.000 Ölçekli Türkiye Jeoloji Haritaları, No.115, Jeoloji Etütleri Daire Başkanlığı, Maden Tetkik ve Arama Genel Müdürlüğü, Ankara.
28. Yalçın, C. (2018). Geology and formation of the Gökçedoğan (Kargı-Çorum) Cu ± Zn mineralization. PhD Thesis, İstanbul University, Institute of Graduate Studies in Science and Engineering, 301.
29. Yalçın, C., Haniçlı, N., Kumral, M., & Kaya, M. (2022). Formation and Tectonic Evolution of Structural Slices in Eastern Kargı Massif (Çorum, Turkey). *Bulletin of the Mineral Research and Exploration*. Doi: 10.19111/bulletinofmre.1067604.
30. Marroni, M., Frassi, C., Göncüoğlu, M. C., Di Vincenzo, G., Pandolfi, L., Rebay, G., ... & Ottria, G. (2014). Late Jurassic amphibolite-facies metamorphism in the Intra-Pontide Suture Zone (Turkey): an eastward extension of the Vardar Ocean from the Balkans into Anatolia?. *Journal of the Geological Society*, 171(5), 605-608.
31. Okay, A. I., Sunal, G., Sherlock, S., Alt ner, D., Tüysüz, O., Kylander-Clark, A. R., & Aygül, M. (2013). Early Cretaceous sedimentation and orogeny on the active margin of Eurasia: Southern Central Pontides, Turkey. *Tectonics*, 32(5), 1247-1271.
32. Okay, A. I., & Nikishin, A. M. (2015). Tectonic evolution of the southern margin of Laurasia in the Black Sea region. *International Geology Review*, 57(5-8), 1051-1076.
33. Aygül, M., Okay, A. I., Oberhänsli, R., & Sudo, M. (2016). Pre-collisional accretionary growth of the southern Laurasian active margin, Central Pontides, Turkey. *Tectonophysics*, 671, 218-234.
34. Günay, K., Dönmez, C., Oyan, V., Yıldırım, N., Çiftçi, E., Yıldız, H., & Özküçük, S. (2018). Geology and geochemistry of sediment-hosted Hanönü massive sulfide deposit (Kastamonu–Turkey). *Ore Geology Reviews*, 101, 652-674.
35. Yılmaz, Y. & Tüysüz, O. (1984). Kastamonu-Boyabat-Vezirköprü-Tosya arasındaki bölgenin jeolojisi (Ilgaz-Kargı masiflerinin etüdü), Maden Tetkik ve Arama Raporu, Maden Tetkik ve Arama Yayınları, Ankara.

36. Folk, R. L. (1962). Spectral subdivision of limestone types in classification of carbonate rocks, W.E. Ham. (ed), AAPG Bull., 1, 62-82.
37. Sun, S. S., & McDonough, W.F., (1989). Chemical and isotopic systematics of oceanic basalts: implications for mantle composition and processes, Geological Society, London, Special Publications, 42, 313-345.
38. Boynton, W. V. (1984). Cosmochemistry of the rare earth elements: meteorite studies. In *Developments in geochemistry* (Vol. 2, pp. 63-114). Elsevier.
39. Elderfield, H., & Greaves, M. J. (1982). The rare earth elements in seawater. *Nature*, 296(5854), 214-219. <https://doi.org/10.1038/296214a0>.
40. Piper, D. Z. (1974). Rare earth elements in the sedimentary cycle: a summary. *Chemical geology*, 14(4), 285-304. [https://doi.org/10.1016/0009-2541\(74\)90066-7](https://doi.org/10.1016/0009-2541(74)90066-7).
41. German, C.R., & Elderfield, H. (1989). Rare earth elements in Saanich Inlet, British Columbia, a seasonally anoxic basin. *Geochimica et Cosmochimica Acta*, 53 (10), 2561-2571. [https://doi.org/10.1016/0016-7037\(89\)90128-2](https://doi.org/10.1016/0016-7037(89)90128-2).
42. Roser, B. P., & Korsch, R. J. (1988). Provenance signatures of sandstone-mudstone suites determined using discriminant function analysis of major-element data. *Chemical geology*, 67(1-2), 119-139.
43. Suttner, L. J., & Dutta, P. K. (1986). Alluvial sandstone composition and paleoclimate; I, Framework mineralogy. *Journal of Sedimentary Research*, 56(3), 329-345.
44. Condie, K. C. (1993). Chemical composition and evolution of the upper continental crust: contrasting results from surface samples and shales. *Chemical geology*, 104(1-4), 1-37.
45. Cullers, R. L. (1995). The controls on the major- and trace-element evolution of shales, siltstones and sandstones of Ordovician to Tertiary age in the Wet Mountains region, Colorado, USA. *Chemical Geology*, 123(1-4), 107-131.
46. Cullers, R. L., & Podkovyrov, V. N. (2002). The source and origin of terrigenous sedimentary rocks in the Mesoproterozoic Uj group, southeastern Russia. *Precambrian Research*, 117(3-4), 157-183. [http://dx.doi.org/10.1016/S0301-9268\(02\)00079-7](http://dx.doi.org/10.1016/S0301-9268(02)00079-7).
47. Yalçın, C., Hanilçi, N., Kumral, M., & Kaya, M. (2022). Petrographic and geochemical characterization of sandstones in upper level of ophiolitic melange in Central Pontides. *Advanced Engineering Days (AED)*, 4, 96-99.



© Author(s) 2022. This work is distributed under <https://creativecommons.org/licenses/by-sa/4.0/>